

# Preparation and characterisation of activated Ni (Mn)/Mg/Al hydrotalcites for combustion catalysis

Květa Jirátová<sup>a,\*</sup>, Pavel Čuba<sup>a</sup>, František Kovanda<sup>b</sup>,  
Lionel Hilaire<sup>c</sup>, Véronique Pitchon<sup>c</sup>

<sup>a</sup> Institute of Chemical Process Fundamentals CAS, Rozvojová 135, 165 02 Prague, Czech Republic

<sup>b</sup> Department of Solid State Chemistry, Institute of Chemical Technology, Technická 5, 166 28 Prague, Czech Republic

<sup>c</sup> LMSPC, Laboratoire des Matériaux, Surfaces et Procédés pour la Catalyse, UMR 7515 du CNRS-ECPM,  
25 rue Becquerel, 67087 Strasbourg Cedex 2, France

## Abstract

The Ni–Mg–Al and Mg–Mn–Al hydrotalcite-like compounds with various Ni and Mn contents (molar ratios Ni:Mg:Al in hydroxide layers of 4:0:2, 3:1:2, and 2:2:2 and Mg:Mn:Al of 4:2:0 and 4:1:1, respectively) were prepared by coprecipitation. The products were characterised by chemical analysis and X-ray diffraction (XRD) measurements. After calcination at different temperatures, the properties of the resulting oxides (surface area, porous structure and surface concentration of metals by XPS) were examined. From the catalysts calcined at 800 °C the Ni<sub>4</sub>Al<sub>2</sub> sample showed the highest surface area and the highest catalytic activity. The oxidation activity in methane combustion (related to the surface area of mesopores) depended on the amount of surface nickel or manganese component linearly. The lower activity of manganese over nickel in methane combustion was proved.

© 2002 Elsevier Science B.V. All rights reserved.

**Keywords:** Hydrotalcites; Metal oxide catalysts; Methane combustion

## 1. Introduction

The principal interest of catalytic combustion over flame combustion [1] is the fact that the temperature is considerably lower therefore preventing the reaction between nitrogen and oxygen to form undesirable NO<sub>x</sub>. But the reaction is still performed at temperatures in excess of 1000 °C and therefore, a suitable catalyst should retain high surface area after exposure to high temperatures. Hydrotalcites could be promising materials as they lead, after calcination at high temperatures, to mixed oxides of small

crystallite size, high thermal stability and a large surface area. Hydrotalcite-like compounds, a class of layered double hydroxides, consist of positively charged metal hydroxide layers separated from each other by anions and water molecules. The layers contain metal cations of at least two different oxidation states. The chemical composition of hydrotalcite-like compounds can be represented by the general formula [M<sup>II</sup><sub>1-x</sub>M<sup>III</sup><sub>x</sub>(OH)<sub>2</sub>]<sup>x+</sup>[A<sup>n-</sup><sub>x/n</sub> · yH<sub>2</sub>O]<sup>x-</sup> where M<sup>II</sup> and M<sup>III</sup> are divalent and trivalent metal ions, A<sup>n-</sup> is an *n*-valent anion, and *x* can have values between approximately 0.25 and 0.33. Their structure is similar to that of brucite–Mg(OH)<sub>2</sub> where each Mg<sup>2+</sup> ion is octahedrally surrounded by six OH<sup>-</sup> ions and the different octahedra share edges to form infinite

\* Corresponding author.

E-mail address: jiratova@icpf.cas.cz (K. Jirátová).

sheets. The sheets are stacked one on top of the other and are held together by weak interactions via hydrogen bonds. In the hydrotalcite-like compounds, the  $M^{II}/M^{III}$  isomorphous substitution in octahedral sites of the hydroxide sheet results in a net positive charge which is neutralised by the interlayers composed of anions and water molecules [2,3]. Hydrotalcite-like compounds as prepared or after calcination at high temperatures have found many practical applications. They are often used as catalysts or catalyst precursors, ion exchangers, adsorbents, polymer stabilisers, etc. Many catalysts based on mixed oxides can be obtained by a controlled decomposition of the hydrotalcite-like compounds [4,5]. These catalysts show a large surface area, basic properties, high metal dispersion, and stability against sintering.

Many hydrotalcite-like compounds with various combinations of  $M^{II}$  and  $M^{III}$  metal cations in hydroxide layers can be prepared by coprecipitation. Thus, precursors with desired and well-defined content of metal cations can be obtained. As it is known that some metal oxides (Cr, Mn, Ni, Cu, Fe, etc.) are active in catalytic combustion we tested a set of calcined Ni–Mg–Al and Mg–Mn–Al hydrotalcite-like compounds (with Ni:Mg:Al molar ratio of 4:0:2, 3:1:2 and 2:2:2 and Mg:Mn:Al molar ratio of 4:2:0 and 4:1:1, respectively) in methane combustion.

The presented work deals with the characterisation of the physical–chemical properties of nickel and manganese containing hydrotalcite-like precursors and of mixed oxides prepared by their calcination. The aim was to carry out an investigation of the characteristics of the calcined Ni–Mg–Al and Mg–Mn–Al hydrotalcite-like compounds, to evaluate the effect of the calcination temperature on their physical properties and to find out their activity in combustion of methane.

## 2. Experimental methods

### 2.1. Hydrotalcite preparation

Samples of Ni–Mg–Al hydrotalcite-like compounds with Ni:Mg:Al molar ratios of 4:0:2, 3:1:2 and 2:2:2 (assigned as  $Ni_4Al_2$ ,  $Ni_3MgAl_2$  and  $Ni_2Mg_2Al_2$ , respectively) and Mg–Mn–Al hydrotalcite-like compounds with Mg:Mn:Al molar ratios of 4:2:0 and

4:1:1 (assigned as  $Mg_4Mn_2$  and  $Mg_4MnAl$ , respectively) were prepared by coprecipitation. An aqueous solution (200 ml) containing appropriate amounts of  $NiSO_4 \cdot 7H_2O$  or  $MnSO_4 \cdot 7H_2O$ ,  $MgSO_4 \cdot 7H_2O$  and  $Al_2(SO_4)_3 \cdot 18H_2O$  with total metal ion concentration of  $1.5 \text{ mol l}^{-1}$  was added dropwise with vigorous stirring into 200 ml of 0.5 M  $Na_2CO_3$  solution. The addition took about 1 h. In the course of synthesis, the temperature was maintained at 30 °C and pH at about 10 by a simultaneous addition of a 3 M NaOH solution. The resulting suspension was then maintained at 30 °C, with stirring, for 18 h. The product was filtered off and washed several times with distilled water and dried overnight at 60 °C in air. The predried precursors were dried at 130 °C and calcined at 800 °C for 2 h, unless otherwise mentioned.

### 2.2. Characterisation of the products

#### 2.2.1. X-ray diffraction (XRD)

Powder XRD patterns were recorded using a Seifert XRD 3000P instrument with Co  $K\alpha$  radiation ( $\lambda = 0.179026 \text{ nm}$ , graphite monochromator, goniometer with Bragg–Brentano geometry) in  $2\theta$  range 12–75°, step size 0.05°.

#### 2.2.2. Surface area and pore size measurements

The surface area of the dried/calcined materials was determined by one-point BET method after activation of the samples by their heating (0.5 h) at the chosen calcination temperature. A more precise determination of surface area of the catalysts calcined at 800 °C was obtained from nitrogen adsorption–desorption isotherms, which were obtained after evacuation at 350 °C and 1 Pa for 5 h in ASAP 2100M (Micromeritics, USA). The data were analysed using BJH theoretical model. Apart from mesopores, the presence of micropores was identified and their volume calculated by the  $V-t$  method. The micropore volume  $V_{\text{micro}}$  was determined as the volume at layer thickness equal to zero from the plot of adsorbed nitrogen volume versus thickness of the adsorbed layer.

#### 2.2.3. XPS measurements

XPS spectra of the catalysts calcined at 800 °C were taken with a Vacuum Generators ESCA 3 apparatus using the Mg  $K\alpha$  radiation as X-ray source. The binding energies of the photoemitted electrons were

corrected from charge effects by calibration with respect to the signal of the adventitious C 1s at 284.8 eV. Surface compositions were determined using the usual ionisation cross sections tabulated by Scofield [8] and we compared the intensities of the Mg 2p, Ni 3p and Al 2p levels in order to avoid corrections from the escape depths and the analyser transmission. Curve fitting analysis of the slightly overlapping Ni 3p and Al 2p peaks was performed using a Doniach–Sunjic routine with no asymmetry parameter.

#### 2.2.4. Catalytic measurements

A standard test was developed in order to evaluate the intrinsic activities of the catalyst and to locate the zone of temperature suitable for kinetics measurements, i.e. where conversion is lower than 20%. The methane combustion activity was determined at atmospheric pressure using a fixed bed quartz micro-reactor packed with 0.50 g of a catalyst and with the same amount of inert cordierite. A mixture containing 1% CH<sub>4</sub> and 4% O<sub>2</sub> (He as eluent gas) with a flow rate of 75 cm<sup>3</sup> min<sup>−1</sup> was used. The flow was adjusted by means of Tylan flow controllers. The test was proven perfectly repeatable after two runs. The analysis was performed by means of an on-line GC using Porapak-Q column for methane and by Rosemount infrared analysers for both CO and CO<sub>2</sub>. In certain cases, traces of CO at high conversion with a concentration lower than 30 ppm were detected which was considered negligible for the rate calculations.

For the kinetics measurement of order to methane, its partial pressure was varied between 3.8 and 18.8 Torr and the partial pressure of oxygen was varied

between 22.8 and 114 Torr. In all cases, the stoichiometry between methane and oxygen was kept above two (stoichiometric and overstoichiometric). Experiments were carried out at four different temperatures for each catalyst in the range 500–615 °C. The average temperature for a particular catalyst was ca. 100 °C for reliable evaluation of kinetic parameters temperature dependence. The reactor temperature was monitored continuously by a thermocouple; the catalyst temperature was constant within ±1 °C. Methane conversion rate per unit of catalyst mass could thus be measured as a function of the temperature and the partial pressure calculated on the basis of mass balance. Each measurement was repeated six times with reproducibility better than ±3%. In addition, one standard set of reaction conditions was routinely repeated at the end of experiments to ensure that the catalyst had not sustained any long-term loss of activity. The catalytic system was found to operate with negligible diffusion retardation of the reaction rate; heat transport effects can also be disregarded.

### 3. Results and discussion

#### 3.1. Catalyst composition

The compositions of the precipitated dried solids are presented in Table 1. The data show that prepared dried materials have main components in amounts very close to intended. All catalysts also show sodium in amounts of 0.02–1.55 wt.% and higher amounts of sulphates

Table 1  
Chemical composition of Ni–Mg–Al and Mg–Mn–Al hydrotalcite-like precursors dried at 60 °C<sup>a</sup>

Sample	Chemical analysis <sup>a</sup> (wt.%)					Molar ratio			
	Ni (Mn)	Mg	Al	Na	SO <sub>4</sub> <sup>2−</sup>	Ni/Al (Mn/Mg)		Mg/Al	
						Int. <sup>b</sup>	Calc. <sup>c</sup>	Int. <sup>b</sup>	Calc. <sup>c</sup>
Ni <sub>4</sub> Al <sub>2</sub>	32.2	0	7.53	0.38	5.89	2	1.97	0	0
Ni <sub>3</sub> MgAl <sub>2</sub>	31.66	4.04	10.06	0.03	7.53	1.5	1.445	0.5	0.445
Ni <sub>2</sub> Mg <sub>2</sub> Al <sub>2</sub>	22.68	8.38	10.75	0.02	9.38	1	0.97	1	0.865
Mg <sub>4</sub> Mn <sub>2</sub>	18.6	17.4	0	1.45	2.15	0.5	0.474	–	–
Mg <sub>4</sub> MnAl	8.1	14.7	4.67	1.55	5.0	0.25	0.243	4.0	3.50

<sup>a</sup> Rest to 100% is water and CO<sub>2</sub>.

<sup>b</sup> Intended.

<sup>c</sup> Calculated from analysis.

that remained in the catalysts from initial compounds used during the synthesis of hydrotalcites.

### 3.2. XRD and SEM analysis

The dried Ni–Mg–Al samples exhibited diffraction patterns characteristic for hydrotalcite-like compounds but their crystallinity seems to be relatively poor, as the diffraction peaks were wide and low. The powder XRD patterns of the  $\text{Ni}_4\text{Al}_2$  and  $\text{Ni}_2\text{Mg}_2\text{Al}_2$  samples as a function of calcination temperature are shown in Fig. 1a and b. The  $\text{Ni}_4\text{Al}_2$  sample calcined at 200 °C still exhibited the layered hydrotalcite crystal structure but after calcination at 300 °C it was rather amorphous (see Fig. 1a). Thermal analysis (TG/DTA) confirmed the loss of interlayer crystal water (dehydration) at 120–200 °C and sample decomposition at about 360 °C. Thermal decomposition was accompanied by dehydroxylation and carbon dioxide evolution and the layered crystal structure of hydrotalcite collapsed to form Ni and Al oxides. A starting crystallisation of NiO (bunsenite) was detected in powder XRD pattern of the sample calcined at 400 °C. Higher calcination temperature enhanced the crystallisation of NiO. Together with bunsenite, the  $\text{NiAl}_2\text{O}_4$  spinel was detected in powder XRD patterns of the samples calcined at 900 °C and higher temperatures.

Thermal behaviour of  $\text{Ni}_2\text{Mg}_2\text{Al}_2$  sample was similar to that of  $\text{Ni}_4\text{Al}_2$  sample. Magnesium containing oxides—MgO (periclase) and  $\text{MgAl}_2\text{O}_4$  spinel were detected in powder XRD patterns of calcined samples together with NiO and  $\text{NiAl}_2\text{O}_4$  (see Fig. 1b). The dehydration and decomposition temperatures observed in DTA curve of  $\text{Ni}_2\text{Mg}_2\text{Al}_2$  sample were a little higher in comparison with  $\text{Ni}_4\text{Al}_2$  sample (140 and 390 °C, respectively).

The powder XRD pattern of the prepared Mg–Mn precursor dried at 60 °C showed a well-crystallised hydrotalcite-like phase (Fig. 1c). The crystallinity of the sample calcined at 200 °C was very poor but the hydrotalcite peaks could be still detected. The sample calcined at 300 °C was quite amorphous. TG and DTA measurements confirmed the sample dehydration at ca. 180 °C and the sample decomposition at about 290 °C. Crystallisation of oxides,  $\text{Mn}_3\text{O}_4$  (hausmannite) and MgO (periclase), was observed at 400 °C and higher temperatures. The  $\text{Mg}_2\text{MnO}_4$  spinel appeared together with these oxides in powder XRD patterns

when the sample was calcined at 800 °C and higher temperatures.

The SEM microphotographs of  $\text{Ni}_4\text{Al}_2$  hydrotalcite dried at 60 °C and of the same sample calcined at 450, 800 and 1150 °C are given in Fig. 2. The microphotograph of the dried sample showed relative compact particles formed by aggregation of small primary crystals. After calcination at 450 °C the sample was already decomposed. The surface of the observed particles was broken up and more open in comparison with non-calcined sample. Calcination at high temperatures caused a crystallisation of oxide phases (bunsenite and  $\text{NiAl}_2\text{O}_4$  spinel). The grain structure of particles formed by agglomeration of oxide crystals can be seen in the microphotograph of the sample calcined at 1150 °C. The other samples were not studied by SEM.

### 3.3. Surface area and porous structure of calcined hydrotalcite-like compounds

The effect of calcination temperature on the surface area of the prepared hydrotalcite-like compounds can be seen in Table 2 and Fig. 3. Hydrotalcite-like compounds dried at 130 °C exhibited relatively low surface areas. The dried Mg–Mn–(Al) hydrotalcite-like compounds show higher surface areas ( $51\text{--}90\text{ m}^2\text{ g}^{-1}$ ) than Ni–(Mg)–Al samples ( $15\text{--}23\text{ m}^2\text{ g}^{-1}$ ), though crystallinity of the Mg–Mn–(Al) samples is higher (Figs. 1a and c). With increasing calcination temperature of hydrotalcite-like compounds the surface area was increasing until a maximum surface area was achieved (around 450 °C). Further increase in calcination temperature caused a decrease in the surface area. The  $\text{Ni}_4\text{Al}_2$  sample when calcined at 800 °C showed the highest surface area ( $88\text{ m}^2\text{ g}^{-1}$ ). At the same calcination temperature we observed a decrease in surface area with decreasing nickel content in the Ni–Mg–Al hydrotalcite-like precursors ( $\text{Ni}_2\text{Mg}_2\text{Al}_2$  sample shows only half of the value).

The Mg–Mn–(Al) samples calcined at 800 °C showed surface area of five to seven times lower than the Ni–(Mg)–Al samples, though the surface area of the Mg–Mn–(Al) hydrotalcite-like compounds dried at 130 °C was exactly opposite (two to six times higher). This phenomenon can be connected with different temperature stability of the compounds arising during calcination (Table 3). A sharp increase in the

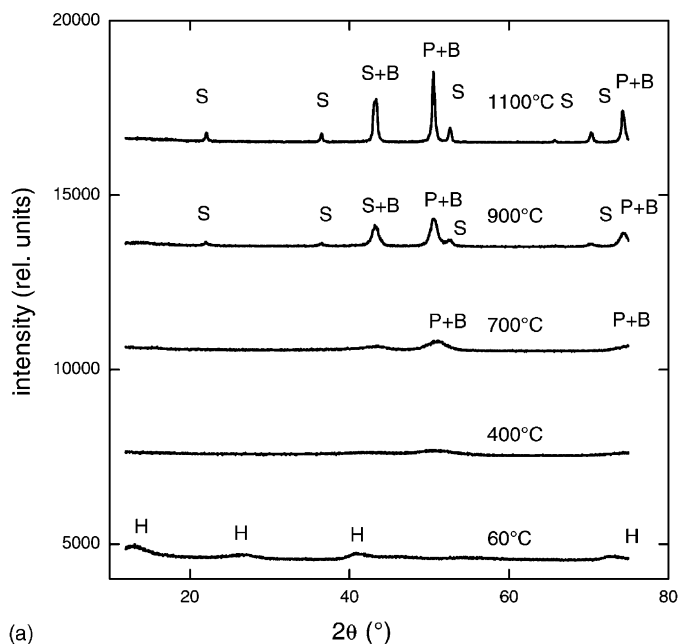
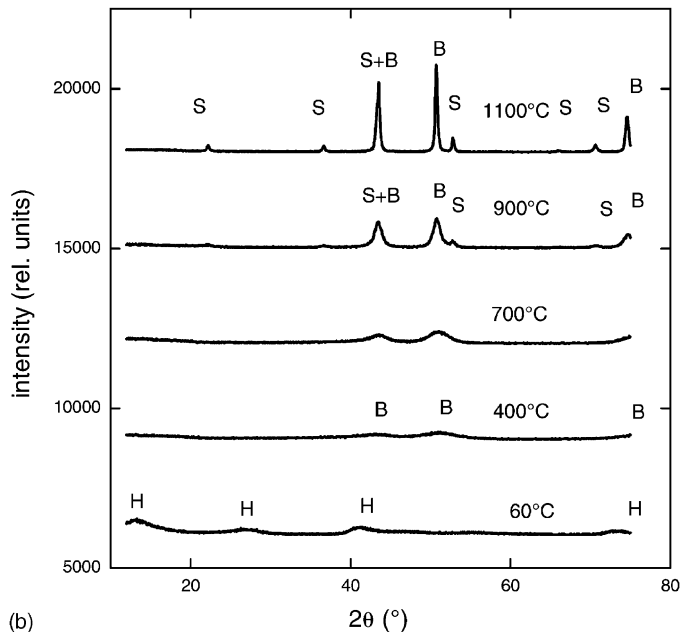
**Ni<sub>2</sub>Mg<sub>2</sub>Al<sub>2</sub>****Ni<sub>4</sub>Al<sub>2</sub>**

Fig. 1. Powder XRD patterns of Ni–Al, Ni–Mg–Al and Mg–Mn hydrotalcite-like compounds as a function of calcination temperature: (a) Ni<sub>4</sub>Al<sub>2</sub> sample—H: hydrotalcite, B: bunsenite (NiO), S: spinel (Ni<sub>2</sub>AlO<sub>4</sub>); (b) Ni<sub>2</sub>Mg<sub>2</sub>Al<sub>2</sub> sample—H: hydrotalcite, B: bunsenite (NiO), P: periclase, S: spinel (Ni<sub>2</sub>AlO<sub>4</sub> and/or MgAl<sub>2</sub>O<sub>4</sub>); (c) Mg<sub>4</sub>Mn<sub>2</sub> sample—H: hydrotalcite, O: hausmannite (Mn<sub>3</sub>O<sub>4</sub>), P: periclase (MgO), S: spinel (Mg<sub>2</sub>MnO<sub>4</sub>).

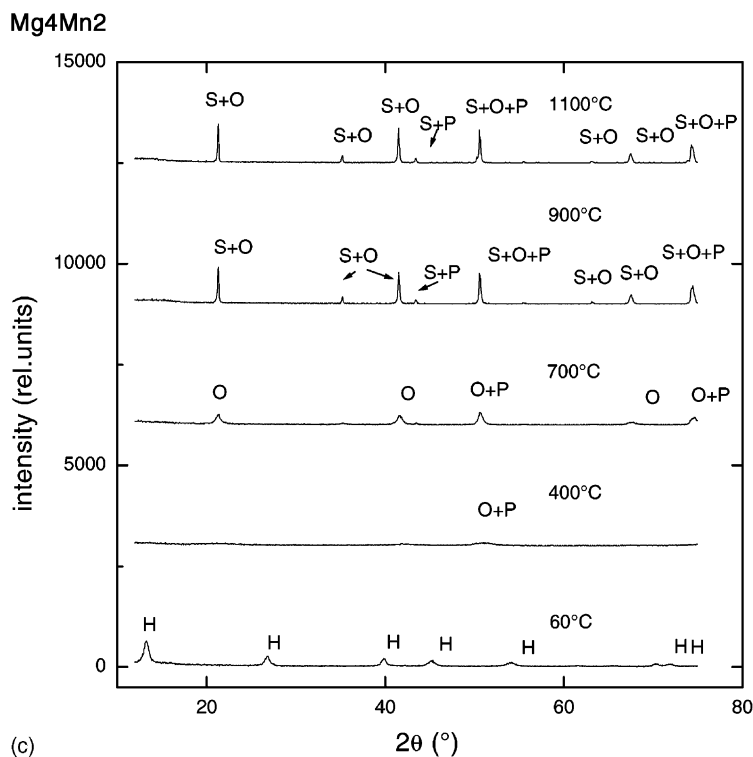


Fig. 1. (Continued).

surface area accompanying the thermal decomposition of hydrotalcite-like compounds is usually observed during their heating. Samples calcined at temperatures close to the decomposition temperatures exhibit a maximum value of surface area and it decreases with further increasing calcination temperature. This fact can explain the lower surface area values found for

Mg–Mn–(Al) samples at 450 °C in comparison with Ni–(Mg)–Al samples as the thermal decomposition of Mg–Mn–(Al) samples occurred at lower calcination temperatures than that of Ni–(Mg)–Al samples.

Surface area of the hydrotalcites-like compounds calcined at 800 °C was examined more deeply from physical sorption of nitrogen. Adsorption–desorption

Table 2

Characteristics of the porous structure of the catalysts calcined at various temperatures<sup>a</sup>

Catalyst	Calcination temperature (°C)					
	130	450	650	800		
	$S_{\text{BET}}$ (m <sup>2</sup> g <sup>-1</sup> )	$S_{\text{BET}}$ (m <sup>2</sup> g <sup>-1</sup> )	$S_{\text{BET}}$ (m <sup>2</sup> g <sup>-1</sup> )	$S_{\text{BET}}$ (m <sup>2</sup> g <sup>-1</sup> )	$S_{\text{meso}}$ (m <sup>2</sup> g <sup>-1</sup> )	$V_{\text{micro}}$ (mm <sup>3</sup> g <sup>-1</sup> )
Ni <sub>4</sub> Al <sub>2</sub>	15	267	157	88	59.8	25.7
Ni <sub>3</sub> MgAl <sub>2</sub>	22	254	136	60	34.2	17.0
Ni <sub>2</sub> Mg <sub>2</sub> Al <sub>2</sub>	23	192	114	45	26.5	13.2
Mg <sub>4</sub> Mn <sub>2</sub>	90	142	37	16	6.5	5.2
Mg <sub>4</sub> MnAl	51	174	98	12	4.9	3.8

<sup>a</sup>  $S_{\text{BET}}$  is the surface area determined from BET equation,  $S_{\text{meso}}$  the surface area of mesopores with diameter  $d > 1.5$  nm, and  $V_{\text{micro}}$  is the volume of micropores with diameter  $< 1.5$  nm given as volume of liquid nitrogen.



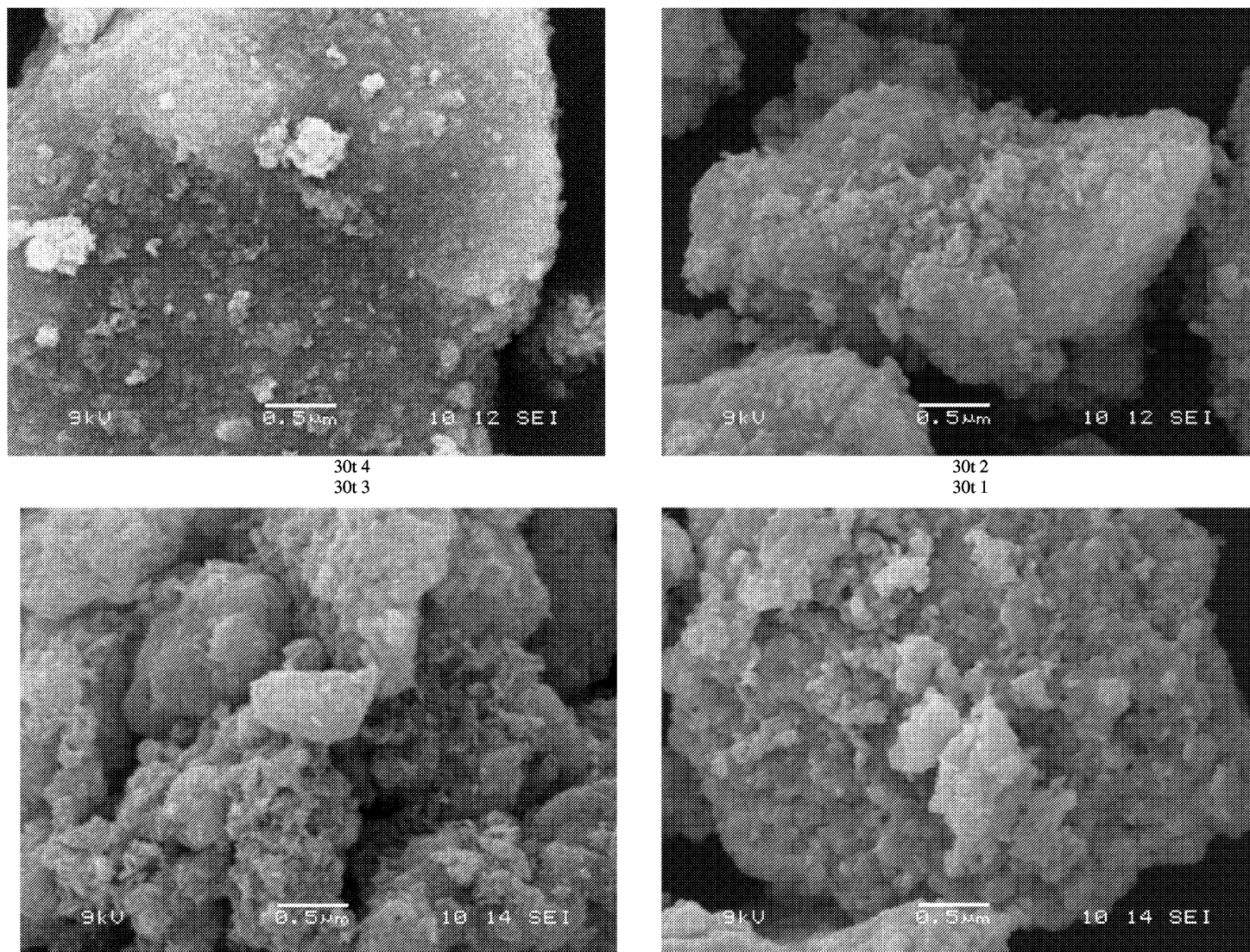


Fig. 2. SEM microphotographs of  $\text{Ni}_4\text{Al}_2$  hydrotalcite-like compounds dried at  $60^\circ\text{C}$  and calcined at  $450$ ,  $800$  and  $1150^\circ\text{C}$ .

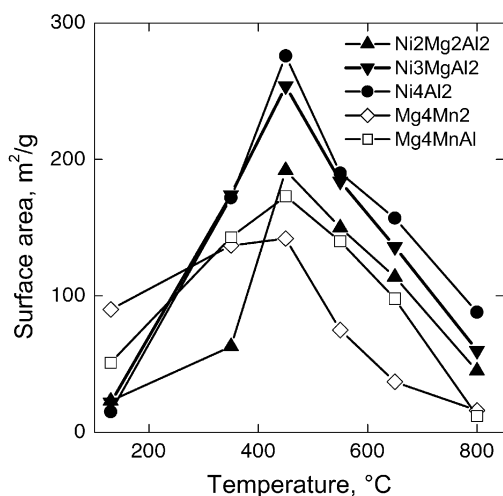


Fig. 3. Surface area of the catalytic systems (determined by one-point BET method) as a function of calcination temperature.

isotherms of nitrogen exhibited the IV + I type of shape (according to IUPAC classification). An example of the adsorption–desorption isotherms for  $\text{Ni}_4\text{Al}_2$  sample can be seen in Fig. 4. A rapid increase in the amount of adsorbed nitrogen in the range of very low relative pressures is an indication of the presence of micropores (pores with radii less than 2 nm according to IUPAC), and it means that the samples contain both micropores and mesopores. In such a case, the use of the classic BET method causes overestimation of the  $C$  constant (the equilibrium constant of adsorption in the first adsorption layer at the measuring temperature in BET equation describing multilayer adsorption) and incorrectly high specific surfaces. For that reason, volume of micropores was calculated by the

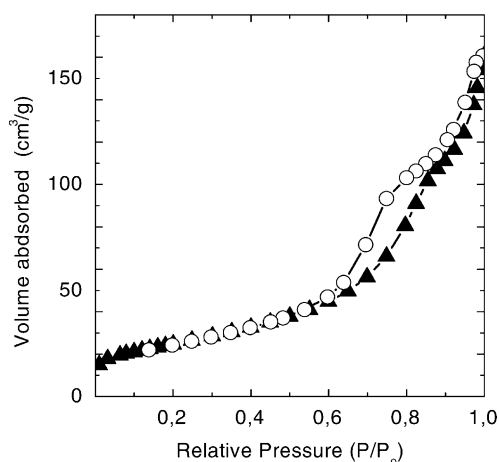


Fig. 4. Adsorption–desorption isotherms of nitrogen at  $-195^\circ\text{C}$  taken with the  $\text{Ni}_4\text{Al}_2$  catalyst calcined at  $800^\circ\text{C}$ .

$V-t$  method (equals to the volume obtained from the plot of adsorbed nitrogen volume versus thickness of the adsorbed layer at layer thickness equal to zero). Then, specific surfaces of mesopores were determined by three-parameter non-linear fitting of experimental adsorption points in the BET region proposed by Schneider [6]. The data are summarised in Table 2. It can be seen that calcination of the hydrotalcite-like precursors even to  $800^\circ\text{C}$  preserves some amount of micropores, though their proportion in the total pore volume is not very high. The  $C$  constants found for all samples calcined at  $800^\circ\text{C}$  moved within limits 4–9, what indicates a similarity in the porous structure of the samples.

Compared to the Ni–(Mg)–Al system the Mg–Mn–(Al) calcined hydrotalcite-like compounds show lower values of both,  $S_{\text{meso}}$  and  $V_{\text{micro}}$ .

Table 3

Melting points of compounds arising during calcination of hydrotalcite-like compounds

	Catalytic system	
	Ni–(Mg)–Al	Mg–Mn–(Al)
Oxide		
Compound	NiO	$\text{Mn}_3\text{O}_4$
Melting points ( $^\circ\text{C}$ )	1990	1705
Spinel [7]		
Compound	$\text{NiAl}_2\text{O}_4$	$\text{Mg}_2\text{MnO}_4$
Melting points ( $^\circ\text{C}$ )	2110	1550

### 3.4. Catalytic activity in methane combustion

The catalyst calcined at  $800^\circ\text{C}$  were used in combustion of methane. Methane conversions as a function of reaction temperature are given in Fig. 5. In the temperature range  $300$ – $900^\circ\text{C}$  the  $\text{Mg}_4\text{MnAl}$  system was completely inactive, while  $\text{Mg}_4\text{Mn}_2$  system showed some activity, though relatively low. The catalysts having nickel as an active component were much more active. With these systems, methane conversions observed at  $650^\circ\text{C}$  (Table 4) moved between 38%



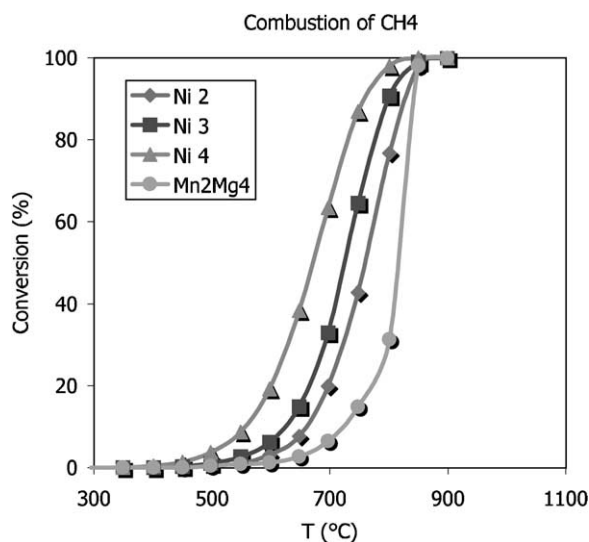


Fig. 5. Catalytic activities of the hydrotalcite-like compounds (calcined at 800 °C) in methane combustion.

(Ni<sub>4</sub>Al<sub>2</sub>) and 7% (Ni<sub>2</sub>Mg<sub>2</sub>Al<sub>2</sub>). With all catalysts, the reaction rates calculated per 1 g of the catalysts varied in the range 0–1428 mmol h<sup>-1</sup> g<sup>-1</sup>.

Kinetic analysis carried out in the temperature range 500–615 °C with the most active Ni<sub>4</sub>Al<sub>2</sub> catalyst gave the following data: rate constant 16 mmol h<sup>-1</sup> m<sub>BET</sub><sup>-2</sup>, order to methane 0.5, order to oxygen 0.35 and activation energy 84.85 kJ mol<sup>-1</sup>.

### 3.5. XPS study of catalysts

XPS measurements enabled us to analyse the surface concentration of active components, Ni or Mn, in various stages of the catalyst use. XPS spectra of Ni 3p and Al 2p are shown in Fig. 6. Calculated molar

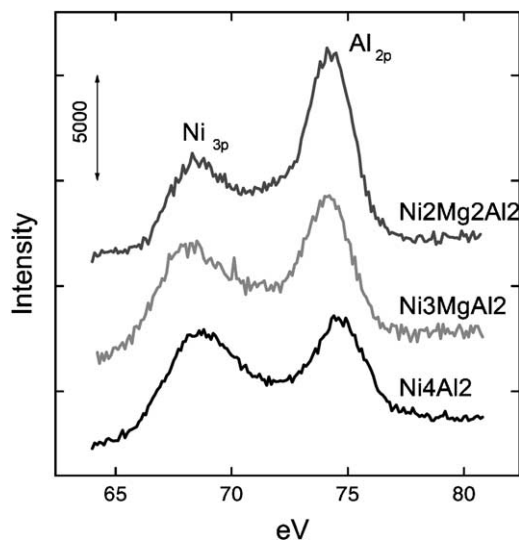


Fig. 6. XPS patterns of the Ni-(Mg)-Al catalysts.

ratios of Ni to Al or Mn to Mg taken before and after the catalytic tests are given in Table 5. Experimentally determined Ni/Al molar ratios depended linearly on bulk Ni/Al molar ratios, but parameter *B* in a linear regression equation  $y = A + Bx$  is not equal to 1 but 0.25. This comes from the fact that there is a lack of nickel atoms on the surface of all samples belonging to the Ni-Mg-Al system.

A change of surface concentration of active metals with calcination temperature was also studied by XPS for both catalytic systems. Molar ratios of Ni/Al in Ni<sub>4</sub>Al<sub>2</sub> and Mn/Mg in Mg<sub>4</sub>Mn<sub>2</sub> exhibited different behaviour with calcination temperature (Fig. 7). While Mn/Mg molar ratio was increasing with increasing calcination temperature, the Ni/Al molar ratio was slightly decreasing.

Table 4

Methane conversion determined at 650 °C and reaction rates of methane combustion calculated per amount of catalyst per BET surface area and surface area of mesopores

Catalyst	<i>x</i> (%)	Rate (mmol h <sup>-1</sup> g <sup>-1</sup> )	Rate (μmol h <sup>-1</sup> m <sub>BET</sub> <sup>-2</sup> )	Rate (μmol h <sup>-1</sup> m <sub>meso</sub> <sup>-2</sup> )
Ni <sub>4</sub> Al <sub>2</sub>	38	1428	16.2	23.8
Ni <sub>3</sub> MgAl <sub>2</sub>	16	599	10	17.5
Ni <sub>2</sub> Mg <sub>2</sub> Al <sub>2</sub>	7	286	6.4	10.8
Mg <sub>4</sub> Mn <sub>2</sub>	2.7	80	5	12.3
Mg <sub>4</sub> MnAl	0	0	0	0

Table 5

XPS data of the catalysts calcined at 800 °C taken before and after the catalytic tests

Catalyst	Surface molar ratio			
	Ni/Al (Mn/Mg)		Mg/Al	
	Before test	After test	Before test	After test
Ni <sub>4</sub> Al <sub>2</sub>	0.47	0.50	0	0
Ni <sub>3</sub> MgAl <sub>2</sub>	0.37	0.34	0.26	0.22
Ni <sub>2</sub> Mg <sub>2</sub> Al <sub>2</sub>	0.25	0.31	0.78	0.49
Mg <sub>4</sub> Mn <sub>2</sub> <sup>a</sup>	0.29	0	–	–
Mg <sub>4</sub> MnAl	0.19	n.d. <sup>b</sup>	0.45	n.d.

<sup>a</sup> Catalyst calcined at 650 °C.

<sup>b</sup> n.d.: not determined.

Based on the found molar ratios surface concentrations of Ni, Mg, Mn and/or Al were calculated (Table 6). XPS data proved that the surface concentration of nickel is about 50% of the value determined as average concentration for both Ni<sub>4</sub>Al<sub>2</sub> and Ni<sub>3</sub>MgAl<sub>2</sub> catalysts, whereas for the Ni<sub>2</sub>Mg<sub>2</sub>Al<sub>2</sub>, the surface concentration of nickel is 37% of the bulk value only. On the contrary, no difference between surface and bulk concentrations of Mn in Mg<sub>4</sub>Mn<sub>2</sub> catalyst was observed.

On all samples the surface concentration of Al is much higher than expected from the stoichiometries; this reveals a higher mobility towards the surface of aluminium oxide during calcination.

Measurements taken on the fresh and used catalysts (after catalytic reaction) exhibited only non-substantial differences in the found surface concentrations. The reason is, probably, the lower temperature used during the catalytic reaction than that used during the calcination of the fresh catalysts.

Table 6

Bulk concentrations of metals calculated from chemical analysis and experimentally determined surface concentration of metals (mol%) present in both fresh catalysts (calcined at 800 °C) and used catalysts (after the catalytic tests)

Catalyst	[Ni] <sub>s</sub> ([Mn] <sub>s</sub> )			[Al] <sub>s</sub>			[Mg] <sub>s</sub>		
	Bulk	Before test	After test	Bulk	Before test	After test	Bulk	Before test	After test
Ni <sub>4</sub> Al <sub>2</sub>	66.6	32.0	33.3	33.4	68.0	66.7	0	0	0
Ni <sub>3</sub> MgAl <sub>2</sub>	50.0	22.7	21.8	16.6	61.3	64.1	33.4	16	14.1
Ni <sub>2</sub> Mg <sub>2</sub> Al <sub>2</sub>	33.3	12.3	17.2	33.3	49.2	55.6	33.3	38.5	27.2
Mg <sub>4</sub> Mn <sub>2</sub>	33.3	33.0 <sup>a</sup>	n.d. <sup>b</sup>	0	0	0	66.6	67.0 <sup>a</sup>	n.d.
Mg <sub>4</sub> MnAl	13.6	5.6	n.d.	30.3	65.1	n.d.	56	29.3	n.d.

<sup>a</sup> Temperature dependence of Mn/Mg molar ratio was taken into account.

<sup>b</sup> n.d.: not determined.

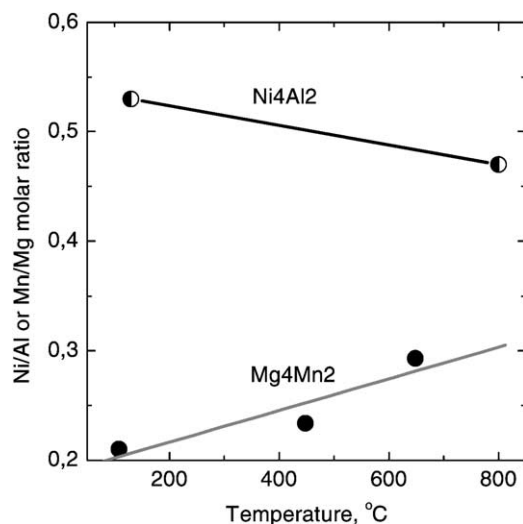


Fig. 7. Surface molar ratios of both Ni/Al in Ni<sub>4</sub>Al<sub>2</sub> catalyst and Mn/Mg in Mg<sub>4</sub>Mn<sub>2</sub> catalyst as a function of calcination temperature of the catalyst.

### 3.6. Correlation of activity in methane combustion and characteristics of the catalysts

We attempted to find a correlation between the catalytic activity in methane combustion and some characteristics of the catalysts. As methane is activated by its contact with the active component, it is understandable that the surface concentration of nickel or manganese is more important than their bulk concentration. Reaction rates calculated per metre square (determined from BET equation) gave a linear dependence on the surface concentration of nickel. The correlation coefficient is 0.983. As we proved, all catalysts calcined at 800 °C possessed some part of micropores

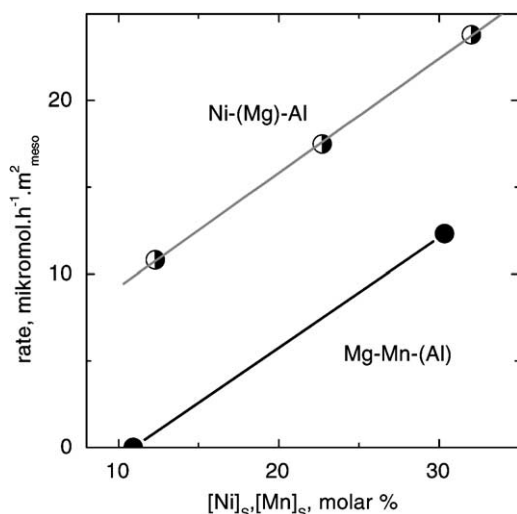


Fig. 8. Relation between rate of methane combustion ( $\mu\text{mol h}^{-1} \text{m}^{-2}$ ), and surface concentrations of nickel or manganese (mol%).

that need not to be accessible to reactant during the catalytic reaction. Therefore we plotted the rates calculated per surface area of mesopores versus surface concentrations of nickel. We obtained a linear dependence with a correlation coefficient of the dependence 0.999. As the correlation is better than that mentioned above, we can judge that combustion of methane proceeds on the surface of mesopores only and the micropores are not accessible.

Reaction rates of methane combustion with Mg–Mn system plotted versus surface concentration of manganese showed similar linear dependence but shifted to lower values (Fig. 8). As it follows from the comparison of both Ni and Mn containing catalysts, the activity of manganese in methane combustion is lower than that of nickel for identical surface metal concentration.

#### 4. Conclusions

1. The accessible surface area plays an important role in methane combustion. Very narrow micropores are probably not important in the reaction.

2. The rate constant of methane combustion calculated per  $S_{\text{meso}}$  increases linearly with increasing amounts of nickel species in the surface layer (determined by XPS). With increasing concentrations of bulk nickel, the concentration of surface nickel species increases non-linearly.
3. X-ray studies proved the presence of spinels in catalytic systems calcined at 800 °C and higher.
4. The high melting point of NiO and  $\text{NiAl}_2\text{O}_4$  probably causes high stability of the surface area during calcination, and therefore high catalytic activity in methane combustion.

#### Acknowledgements

Many thanks are due to Mrs. A. Meens for her help with the XPS experiments. This work was supported by the Czech Ministry of Education, Youth and Sports (research project no. CEZ: MSM 223/10/0002) and by the Grant Agency of Czech Republic (grant no. 106/02/0523).

#### References

- [1] L.D. Pfefferle, L.C. Pfefferle, *Catal. Rev.-Sci. Eng.* 29 (1987) 219.
- [2] A. Vaccari, Preparation and catalytic properties of cationic and anionic clays, *Catal. Today* 41 (1998) 53–71.
- [3] W.T. Reichle, Anionic clay minerals, *CHEMTECH* 16 (1986) 58–63.
- [4] W.T. Reichle, Catalytic reactions by thermally activated synthetic anionic clay materials, *J. Catal.* 94 (1985) 547–557.
- [5] F. Cavani, F. Trifiro, A. Vaccari, Hydrotalcite type anionic clays: preparation, properties and applications, *Catal. Today* 11 (1991) 173–301.
- [6] P. Schneider, Adsorption isotherms of microporous–mesoporous solids revisited, *Appl. Catal. A* 129 (1995) 157–165.
- [7] E.M. Levin, C.R. Robbins, H.F. McMurdie, in: M.K. Reser (Ed.), *Phase Diagrams for Ceramists 1969*, National Bureau of Standards, The American Ceramic Society, Columbus, OH, USA, 1969, p. 47.
- [8] J.H. Scofield, *J. Electron. Spectrosc. Rel. Phenom.* 8 (1976) 129.